Acta Cryst. (1983). A**39**, 825–837

Space-Group Determination by Dynamic Extinction in Convergent-Beam Electron Diffraction

By M. Tanaka, H. Sekii* and T. Nagasawa

Department of Physics, Faculty of Science, Tohoku University, Sendai 980, *Japan*

(*Received* 18 *March* 1983; *accepted* 9 *May* 1983)

Abstract

Tables of dynamic extinction lines which occur in convergent-beam electron diffraction patterns (GM lines) are given for all the space groups on the basis of the rules given by Gjønnes & Moodie [*Acta Cryst.* (1965), **19**, 65–67]. It is found that 191 space groups can be identified by GM lines. A convenient experimental method which distinguishes a screw axis and a glide plane is demonstrated. Experimental results are shown in which the GM lines due to a screw axis and those due to a glide plane are separately observed. The GM lines appearing in a symmetrical four-beam pattern are demonstrated.

Introduction

Dynamic extinction in electron diffraction was first studied by Cowley & Moodie (1959) on the basis of their multi-slice theory. They revealed that dynamic diffraction effects can give no intensity to any kinematically forbidden reflections caused by a screw axis or a glide plane if the incident electron beam impinges exactly parallel to a principal axis of a crystal. Miyake, Takagi & Fujimoto (1960) reinvestigated the problem using Bethe's dynamical theory. They clearly showed the difference between the extinction rules for structure amplitudes and those for reflections, and established the basis to consider the dynamic extinction. As applications of the rules, they gave the following results for the incident beam parallel to a principal axis: A glide plane causes the dynamic extinction in a kinematically forbidden reflection. A twofold screw axis also causes the extinction when only the reflections of the zeroth Laue zone are considered. The kinematically forbidden 200 reflection due to the 4_1 screw axis is dynamically allowed, whereas the 100 reflection is forbidden not only kinematically but also dynamically. The kinematically forbidden reflections not due to symmetry elements but due to special positions, for instance the 222 reflection of the diamond structure, are not forbidden by dynamical diffraction. Cowley, Moodie, Miyake, Takagi & Fujimoto (1961) reconfirmed using the multi-slice method that the kinematically forbidden 200 reflection due to the 4_1 screw axis is allowed by dynamical diffraction when the incident beam is parallel to a principal axis of a crystal. On the basis of a multiple scattering theory (*e.g.* Fujiwara, (1959), Gjønnes & Moodie (1965) revealed the incident-beam orientations at which a kinematically forbidden reflection caused by a glide plane or a twofold screw axis remains forbidden even by dynamical diffraction. They showed that glide planes and twofold screw axes cause the different zero-intensity lines when the reflections of higher Laue zones are taken into account. The zero-intensity lines appearing in convergent-beam electron diffraction (CBED) patterns have been called Gjønnes–Moodie lines (GM lines). Tinnappel (1975) explained the results of Gjønnes & Moodie by applying group theory, his treatment being regarded as an extension of the work of Miyake, Takagi & Fujimoto (1960). Tanaka & Sekii (1982*a*) briefly reported the space-group-determination method using GM lines.

In the present paper, on the basis of the results of Gjønnes & Moodie (1965) and Miyake, Takagi & Fujimoto (1960), we investigate the dynamic extinction rules for the cases when several symmetry elements which cause GM lines coexist and when the symmetry elements are combined with various lattice types. We give tables which list the GM lines expected at various incident-beam directions for all the space groups. We

Table 1. *Dynamic extinction rules for the symmetry elements of a plane-parallel specimen*

Symmetry elements of plane-parallel specimen		Dynamic extinction rules
Glide plane	g	A_2, B_2 and A_3
	g'	Intersection of A and B
Twofold screw axis	$2_1'$	A_2, B_2 and B_3

* Present address: Omron Tateishi Electrics Co, Kyoto 617, Japan.

0108-7673/83/060825-13$01.50

clarify the space groups which can be identified by only the dynamic extinction effect or the GM lines. A convenient experimental method which distinguishes between the GM lines by a glide plane and those by a screw axis is demonstrated. The experimental result in which the GM lines due to a glide plane are separately observed from those due to a screw axis when both symmetry elements coexist is shown. The GM lines appearing in a symmetrical four-beam pattern are demonstrated.

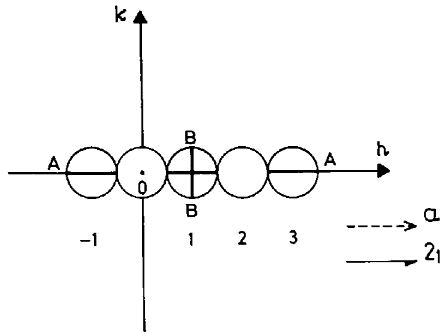

Fig. 1. A and B GM lines in the forbidden reflection disks of a CBED pattern are schematically shown. Directions of the 2_1 screw axis and the glide translation are indicated by solid and dotted arrows, respectively. First-order reflection satisfies Bragg condition.

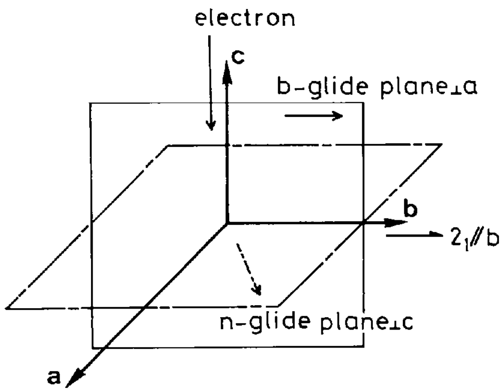

Fig. 2. Geometrical arrangement of the incident beam and symmetry elements to explain rule 6.

Dynamic extinction rules

We consider a perfect crystalline specimen which is plane-parallel and extends infinitely in two dimensions. The specimen has ten point-group symmetry elements

Table 2. *GM lines for point groups* 2, *m and* 2/*m*

Unique axis is in the **b** direction.

Space group	Incident beam direction [h0l]	
3 $P2$		
4 $P2_1$	0k0 2_1	A_2B_2 B_3
5 $C2$		
6 Pm		
7 Pc	h'0l' c	A_2B_2 A_3
8 Cm		
9 Cc	h'0l' c	A_2B_2 A_3
10 $P2/m$		
11 $P2_1/m$	0k0 2_1	A_2B_2 B_3
12 $C2/m$		
13 $P2/c$	h'0l' c	A_2B_2 A_3
14 $P2_1/c$	0k0 2_1 h'0l' c	A_2B_2 B_3 A_2B_2 A_3
15 $C2/c$	h'0l' c	A_2B_2 A_3

Table 3. *GM lines for point group* 222

Space group	Incident beam direction [100]		[010]		[001]		[hk0]		[0kl]		[h0l]	
16 $P222$												
17 $P222_1$	00l 2_1	A_2B_2 B_3	00l 2_1	A_2B_2 B_3			00l 2_1	A_2B_2 B_3				
18 $P2_12_12$	0k0 2_{12}	A_2B_2 B_3	h00 2_{11}	A_2B_2 B_3	h00 2_{11} 0k0 2_{12}	A_2B_2 B_3			h00 2_{11}	A_2B_2 B_3	0k0 2_{12}	A_2B_2 B_3
19 $P2_12_12_1$	0k0 2_{12} 00l 2_{13}	A_2B_2 B_3	h00 2_{11} 00l 2_{13}	A_2B_2 B_3	h00 2_{11} 0k0 2_{12}	A_2B_2 B_3	00l 2_{13}	A_2B_2 B_3	h00 2_{11}	A_2B_2 B_3	0k0 2_{12}	A_2B_2 B_3
20 $C222_1$	00l 2_1	A_2B_2 B_3	00l 2_1	A_2B_2 B_3			00l 2_1	A_2B_2 B_3				
21 $C222$												
22 $F222$												
23 $I222$												
24 $I2_12_12_1$												

which consist of six two-dimensional elements and four three-dimensional ones. The former consists of the 1-, 2-, 3-, 4- and 6-fold rotation axes which are parallel to the surface normal of the specimen and the mirror plane m which includes the surface normal (vertical mirror plane). The latter consists of (1) the mirror plane m' and (2) the twofold axis 2' which are parallel to the specimen surface and pass through the midpoint of the specimen (horizontal mirror plane and horizontal twofold axis), (3) the inversion center i which is placed

Table 4. *GM lines for point group mm2*

Space group	Incident beam direction [100]		[010]		[001]		[$hk0$]		[$0kl$]		[$h0l$]	
25 *Pmm2*												
26 $Pmc2_1$	$00l$ $c, 2_1$	A_2B_2 A_3B_3	$00l$ 2_1	B_3			$00l$ 2_1	A_2B_2 B_3			$h'0l'$ c	A_2B_2 A_3
27 *Pcc2*	$00l$ c_2	A_3	$00l$ c_1	A_3					$0k'l'$ c_1	A_2B_2 A_3	c_2	A_2B_2 A_3
28 *Pma2*					$h00$ a	A_2B_2 A_3					a	A_2B_2 A_3
29 $Pca2_1$	$00l$ 2_1	B_3	$00l$ $c, 2_1$	A_2B_2 A_3B_3	$h00$ a	A_2B_2 A_3	2_1	A_2B_2 B_3	c	A_2B_2 A_3	a	A_2B_2 A_3
30 *Pnc2*	$00l$ c	A_3	$00l$ n	A_3	$0k0$ n	A_2B_2 A_3			n	A_2B_2 A_3	c	A_2B_2 A_3
31 $Pmn2_1$	$00l$ $n, 2_1$	A_2B_2 A_3B_3	$00l$ 2_1	B_3	$h00$ n	A_2B_2 A_3	2_1	A_2B_2 B_3			n	A_2B_2 A_3
32 *Pba2*					$h00$ a $0k0$ b	A_2B_2 A_3			b	A_2B_2 A_3	a	A_2B_2 A_3
33 $Pna2_1$	$00l$ 2_1	B_3	$00l$ $n, 2_1$	A_2B_2 A_3B_3	$h00$ a $0k0$ n	A_2B_2 A_3	2_1	A_2B_2 B_3	n	A_2B_2 A_3	a	A_2B_2 A_3
34 *Pnn2*	$00l$ n_2	A_3	$00l$ n_1	A_3	$h00$ n_2 $0k0$ n_1	A_2B_2 A_3			n_1	A_2B_2 A_3	n_2	A_2B_2 A_3
35 *Cmm2* *ba2*												
36 $Cmc2_1$ $bn2_1$	$00l$ $c, 2_1$	A_2B_2 A_3B_3	$00l$ 2_1	B_3			2_1	A_2B_2 B_3			c	A_2B_2 A_3
37 *Ccc2* *nn2*	$00l$ c_2	A_3	$00l$ c_1	A_3					c_1	A_2B_2 A_3	c_2	A_2B_2 A_3
38 *Amm2* $nc2_1$												
39 *Abm2* $cc2_1$									b	A_2B_2 A_3		
40 *Ama2* $nn2_1$					$h00$ a	A_2B_2 A_3					a	A_2B_2 A_3
41 *Aba2* $cn2_1$					$h00$ a	A_2B_2 A_3			b	A_2B_2 A_3	a	A_2B_2 A_3
42 *Fmm2*												
43 *Fdd2* 2_1	$00l$ $l = 4n + 2$ d_2	A_3	$00l$ $l = 4n + 2$ d_1	A_3	$h00$ $h = 4n + 2$ d_2 $0k0$ $k = 4n + 2$ d_1	A_2B_2 A_3			$k' + l'$ $= 4n + 2$ d_1	A_2B_2 A_3	$h' + l'$ $= 4n + 2$ d_2	A_2B_2 A_3
44 *Imm2* $nn2_1$												
45 *Iba2* $cc2_1$									b	A_2B_2 A_3	a	A_2B_2 A_3
46 *Ima2* $nc2_1$											a	A_2B_2 A_3

Table 5. *GM lines for point group mmm*

Incident beam direction

Space group	[100]		[010]		[001]		[hk0]		[0kl]		[h0l]	
47 $P2/m2/m2/m$												
	$00l$		$00l$		$0k0$							
48 $P2/n2/n2/n$	n_2		n_1		n_1		$h'k'0$	A_2 B_2	$0k'l'$	A_2 B_2	$h'0l'$	A_2 B_2
	$0k0$	A_3	$h00$	A_3	$h00$	A_3	n_3	A_3	n_1	A_3	n_2	A_3
	n_3		n_3		n_2							
49 $P2/c2/c2/m$	$00l$		$00l$						$0k'l'$	A_2 B_2	$h'0l'$	A_2 B_2
	c_2	A_3	c_1	A_3					c_1	A_3	c_2	A_3
					$0k0$							
50 $P2/b2/a2/n$	$0k0$		$h00$		b		$h'k'0$	A_2 B_2	$0k'l'$	A_2 B_2	$h'0l'$	A_2 B_2
	n	A_3	n	A_3	$h00$	A_3	n	A_3	b	A_3	a	A_3
					a							
51 $P2_1/m2/m2/a$			$h00$	A_2 B_2	$h00$		$h'k'0$	A_2 B_2	$h00$	A_2 B_2		
			2_1, a	A_3 B_3	2_1	B_3	a	A_3	2_1	B_3		
	$00l$		$00l$		$0k0$	A_2 B_2					$h'0l'$	A_2 B_2
52 $P2/n2_1/n2/a$	n_2	A_3	n_1		n_1, 2_1	A_3 B_3	$h'k'0$	A_2 B_2	$0k'l'$	A_2 B_2	n_2	A_3
	$0k0$		$h00$	A_3	$h00$		a	A_3	n_1	A_3	$0k0$	A_2 B_2
	2_1	B_3	a		n_2	A_3					2_1	B_3
			$h00$				$h'k'0$	A_2 B_2				
53 $P2/m2/n2_1/a$	$00l$	A_2 B_2	a	A_3	$h00$		a	A_3			$h'0l'$	A_2 B_2
	n, 2_1	A_3 B_3	$00l$		n	A_3	$00l$	A_2 B_2			n	A_3
			2_1	B_3			2_1	B_3				
			$00l$						$0k'l'$	A_2 B_2		
54 $P2_1/c2/c2/a$	$00l$		c_1	A_3	$h00$		$h'k'0$	A_2 B_2	c_1	A_3	$h'0l'$	A_2 B_2
	c_2	A_3	$h00$	A_2 B_2	2_1	B_3	a	A_3	$h00$	A_2 B_2	c_2	A_3
			a, 2_1	A_3 B_3					2_1	B_3		
					$0k0$				$0k'l'$	A_2 B_2	$h'0l'$	A_2 B_2
55 $P2_1/b2_1/a2/m$	$0k0$		$h00$		b, 2_{12}	A_2 B_2			b	A_3	a	A_3
	2_{12}	B_3	2_{11}	B_3	$h00$	A_3 B_3			$h00$	A_2 B_2	$0k0$	A_2 B_2
					a, 2_{11}				2_{11}	B_3	2_{12}	B_3
	$00l$		$00l$		$0k0$				$0k'l'$	A_2 B_2	$h'0l'$	A_2 B_2
56 $P2_1/c2_1/c2/n$	c_2	A_3	c_1	A_3	2_{12}		$h'k'0$	A_2 B_2	c_1	A_3	c_2	A_3
	$0k0$	A_2 B_2	$h00$	A_2 B_2	$h00$	B_3	n	A_3	$h00$	A_2 B_2	$0k0$	A_2 B_2
	2_{12}, n	A_3 B_3	2_{11}, n	A_3 B_3	2_{11}				2_{11}	B_3	2_{12}	B_3
	$00l$	A_2 B_2									$h'0l'$	A_2 B_2
57 $P2/b2_1/c2_1/m$	c, 2_{12}	A_3 B_3	$00l$		$0k0$	A_2 B_2	$00l$	A_2 B_2	$0k'l'$	A_2 B_2	c	A_3
	$0k0$		2_{12}	B_3	b, 2_{11}	A_3 B_3	2_{12}	B_3	b	A_3	$0k0$	A_2 B_2
	2_{11}	B_3									2_{11}	B_3
	$00l$		$00l$		$0k0$				$0k'l'$	A_2 B_2	$h'0l'$	A_2 B_2
58 $P2_1/n2_1/n2/m$	n_2	A_3	n_1	A_3	n_1, 2_{12}	A_2 B_2			n_1	A_3	n_2	A_3
	$0k0$		$h00$		$h00$	A_3 B_3			$h00$	A_2 B_2	$0k0$	A_2 B_2
	2_{12}	B_3	2_{11}	B_3	n_2, 2_{11}				2_{11}	B_3	2_{12}	B_3
					$0k0$							
59 $P2_1/m2_1/m2/n$	$0k0$	A_2 B_2	$h00$	A_2 B_2	2_{12}		$h'k'0$	A_2 B_2	$h00$	A_2 B_2	$0k0$	A_2 B_2
	n, 2_{12}	A_3 B_3	n, 2_{11}	A_3 B_3	$h00$	B_3	n	A_3	2_{11}	B_3	2_{12}	B_3
					2_{11}							
	$00l$	A_2 B_2	$h00$	A_2 B_2	$0k0$		$h'k'0$	A_2 B_2	$0k'l'$	A_2 B_2		
60 $P2_1/b2/c2_1/n$	c, 2_{12}	A_3 B_3	n, 2_{11}	A_3 B_3	b	A_3	n	A_3	b	A_3	$h'0l'$	A_2 B_2
	$0k0$		$00l$		$h00$		$00l$	A_2 B_2	$h00$	A_2 B_2	c	A_3
	n	A_3	2_{12}	B_3	2_{11}	B_3	2_{12}	B_3	2_{11}	B_3		
	$00l$	A_2 B_2	$00l$		$0k0$	A_2 B_2	$h'k'0$	A_2 B_2	$0k'l'$	A_2 B_2	$0k'l'$	A_2 B_2
61 $P2_1/b2_1/c2_1/a$	c, 2_{13}	A_3 B_3	2_{13}	B_3	b, 2_{12}	A_3 B_3	a	A_3	b	A_3	c	A_3
	$0k0$		$h00$	A_2 B_2	$h00$		$00l$	A_2 B_2	$h00$	A_2 B_2	$0k0$	A_2 B_2
	2_{12}	B_3	a, 2_{11}	A_3 B_3	2_{11}	B_3	2_{13}	B_3	2_{11}	B_3	2_{12}	B_3
	$00l$		$00l$		$0k0$	A_2 B_2	$h'k'0$	A_2 B_2	$0k'l'$	A_2 B_2		
62 $P2_1/n2_1/m2_1/a$	2_{11}		n, 2_{13}	A_2 B_2	n, 2_{12}	A_3 B_3	a	A_3	n	A_3	$0k0$	A_2 B_2
	$0k0$	B_3	$h00$	A_3 B_3	$h00$		$00l$	A_2 B_2	$h00$	A_2 B_2	2_{12}	B_3
	2_{12}		a, 2_{11}		2_{11}	B_3	2_{13}	B_3	2_{11}	B_3		
63 $C2/m2/c2_1/m$	$00l$	A_2 B_2	$00l$				$00l$	A_2 B_2			$0k'l'$	A_2 B_2
	c, 2_1	A_3 B_3	2_1	B_3			2_1	B_3			c	A_3
							$h'k'0$	A_2 B_2				
64 $C2/m2/c2_1/a$	$00l$	A_2 B_2	$00l$				a	A_3			$0k'l'$	A_2 B_2
	c, 2_1	A_3 B_3	2_1	B_3			$00l$	A_2 B_2			c	A_3
							2_1	B_3				

Table 5. (*cont.*)

Space group	Incident beam direction											
	[100]		[010]		[001]		[$hk0$]		[$0kl$]		[$h0l$]	
65 $C2/m2/m2/m$												
66 $C2/c2/c2/m$	$00l$ c_2	A_3	$00l$ c_1	A_3					$0k'l'$ c_1	$A_2\ B_2$ A_3	$0k'l'$ c_2	$A_2\ B_2$ A_3
67 $C2/m2/m2/a$							$h'k'0$ a	$A_2\ B_2$ A_3				
68 $C2/c2/c2/a$	$00l$ c_2	A_3	$00l$ c_1	A_3			$h'k'0$ a	$A_2\ B_2$ A_3	$0k'l'$ c_1	$A_2\ B_2$ A_3	$h'0l'$ c_2	$A_2\ B_2$ A_3
69 $F2/m2/m2/m$												
70 $F2/d2/d2/d$	$00l$ $l = 4n + 2$ d_2 $0k0$ $k = 4n + 2$ d_3	A_3	$h00$ $h = 4n + 2$ d_3 $00l$ $l = 4n + 2$ d_1	A_3	$0k0$ $k = 4n + 2$ d_1 $h00$ $h = 4n + 2$ d_2	A_3	$h'k'0$ $h' + k'$ $= 4n + 2$ d_3	$A_2\ B_2$ A_3	$0k'l'$ $k' + l'$ $= 4n + 2$ d_1	$A_2\ B_2$ A_3	$h'0l'$ $h' + l'$ $= 4n + 2$ d_2	$A_2\ B_2$ A_3
71 $I2/m2/m2/m$												
72 $I2/b2/a2/m$									$0k'l'$ b	$A_2\ B_2$ A_3	$h'0l'$ a	$A_2\ B_2$ A_3
73 $I2/b2/c2/a$							$h'k'0$ a	$A_2\ B_2$ A_3	$0k'l'$ b	$A_2\ B_2$ A_3	$h'0l'$ c	$A_2\ B_2$ A_3
74 $I2/m2/m2/a$							$h'k'0$ a	$A_2\ B_2$ A_3				

at the midpoint of the specimen, and (4) the fourfold rotary inversion 4 whose axis is parallel to the surface normal.

Three space-group symmetry elements of the specimen are added to the point-group symmetry elements: (1) the vertical glide plane g whose glide vector is parallel to the specimen surface, (2) the horizontal twofold screw axis $2_1'$ and (3) the horizontal glide plane g', which are related to the point-group elements m, $2'$ and m', respectively. It is noted that the 2_1, 3_1, 3_2..., 6_5 screw axes which are parallel to the surface normal and the vertical glide plane whose glide translation is parallel to the surface normal are not included in the symmetry elements of the specimen.

We summarize the dynamic extinction rules for g, g' and $2_1'$ given by Gjønnes & Moodie (1965) in Table 1 using our notation. The symbols A and B indicate the GM lines as depicted in Fig. 1. The A line runs along the screw axis or the glide translation and through the zone axis of projection. The B line is perpendicular to the A line and at the exact Bragg positions. The suffixes 2 and 3 indicate that the GM lines are formed by the two-dimensional or zeroth Laue-zone interaction and by the three-dimensional or higher Laue-zone interaction, respectively.

Based on the dynamic extinction rules for the symmetry elements g and $2_1'$ of a plane-parallel specimen,* we have investigated the GM line rules expected from the symmetry elements of three-dimensional crystal space groups.

1. When the 2_1, 4_1, 4_3, 6_1, 6_3 and 6_5 screw axes of crystal space groups are set perpendicular to the incident beam, they act as the screw axis $2_1'$ of the plane-parallel specimen, because of the relation $(4_1)^2 = (4_3)^2 = (6_1)^3 = (6_3)^3 = (6_5)^3 = 2_1$. The 4_2, 3_1, 3_2, 6_2 and 6_4 screw axes do not produce GM lines, since the 4_2 axis acts as a twofold axis in the specimen by the relation $(4_2)^2 = 2$, the horizontal threefold screw axis is not included as the symmetry element of the specimen and the 6_2 and 6_4 screw axes are equivalent to 3_1 and 3_2 by the relations $(6_2)^2 = 3_2$ and $(6_4)^2 = 3_1$.

2. When two 2_1 screw axes or the equivalent axes are present perpendicularly, the GM line rules deduced from a single 2_1 screw axis hold for each axis.

3. When the lattice symbol I or F is combined with the 2_1 axis or the equivalent axis, GM lines due to the axis are not formed, since the lattice types prohibit *Umweganregung* of the forbidden reflections due to the screw axis. As a result, for instance space groups $I4$ and $I4_1$ cannot be distinguished by dynamic extinction. The combination of the lattice type A and the 2_1 screw axis in the c direction also produces no GM line. However, the combination does not appear in the standard notation of the space groups.

4. When the glide planes a, b, c, n and d of crystal space groups lie parallel to the incident beam and their glide translations are not parallel to the incident beam, they act as the glide plane g of the plane-parallel specimen. It is noted that the glide translation does not necessarily make a right angle with the incident beam to cause GM lines.

* The dynamic extinction due to g' has been recently observed in the 420 reflection of spinel by Tanaka & Sekii (1982*b*). However, we do not consider the extinction, since it has little advantage in determining the space groups.

5. When the lattice type I or F is combined with the a-, b- or c-glide plane, GM lines due to the plane are not produced in $h00$, $0k0$ and/or $00l$ (h, k and l odd) forbidden reflections, since the lattice types prohibit *Umweganregung* of the forbidden reflections. When the lattice type A is combined with the b or c glide plane in the (100) plane, GM lines due to the plane are not produced in the $0k0$ or $00l$ (k and l odd) reflections,

Table 6. *GM lines for point groups* 4, $\bar{4}$ *and* $4/m$

Space group	Incident beam direction $[hk0]$	
75 $P4$		
76 $P4_1$	$00l$ 4_1	A_2B_2 B_3
77 $P4_2$		
78 $P4_3$	$00l$ 4_3	A_2B_2 B_3
79 $I4$		
80 $I4_1$		
81 $P\bar{4}$		
82 $I\bar{4}$		
83 $P4/m$		
84 $P4_2/m$		
85 $P4/n$	$\bar{k}h0$ n	A_2B_2 A_3
86 $P4_2/n$	$\bar{k}h0$ n	A_2B_2 A_3
87 $I4/m$		
88 $I4_1/a$	$\bar{k}h0$ a	A_2B_2 A_3

Table 7. *GM lines for point group* 422

Space group	Incident beam direction $[hk0]$		$[0kl]$	
89 $P422$				
90 $P42_12$			$h00$ 2_1	A_2B_2 B_3
91 $P4_122$	$00l$ 4_1	A_2B_2 B_3		
92 $P4_12_12$	$00l$ 4_1	A_2B_2 B_3	$h00$ 2_1	A_2B_2 B_3
93 $P4_222$				
94 $P4_22_12$			$h00$ 2_1	A_2B_2 B_3
95 $P4_322$	$00l$ 4_3	A_2B_2 B_3		
96 $P4_32_12$	$00l$ 4_3	A_2B_2 B_3	$h00$ 2_1	A_2B_2 B_3
97 $I422$				
98 $I4_122$				

Table 8. *GM lines for point group* $4mm$

Space group	Incident beam direction $[100]$		$[001]$		$[110]$		$[0kl]$		$[hhl]$	
99 $P4mm$										
100 $P4bm$			$h00$ b_2 $0k0$ b_1	A_2B_2 A_3			$0k'l'$ b	A_2B_2 A_3		
101 $P4_2cm$	$00l$ c_2	A_3					c	A_2B_2 A_3		
102 $P4_2nm$	$00l$ n_2	A_3	$h00$ n_2 $0k0$ n_1	A_2B_2 A_3			n	A_2B_2 A_3		
103 $P4cc$	$00l$ c_{12}	A_3			$00l$ c_2	A_3	c_1	A_2B_2 A_3	$h'h'l'$ c_2	A_2B_2 A_3
104 $P4nc$	$00l$ n_2	A_3	$h00$ n_2 $0k0$ n_1	A_2B_2 A_3	$00l$ c	A_3	n	A_2B_2 A_3	c	A_2B_2 A_3
105 $P4_2mc$					$00l$ c	A_3			c	A_2B_2 A_3
106 $P4_2bc$			$h00$ b_2 $0k0$ b_1	A_2B_2 A_3	$00l$ c	A_3	b	A_2B_2 A_3	c	A_2B_2 A_3
107 $I4mm$										
108 $I4cm$							c	A_2B_2 A_3		
109 $I4_1md$			$hh0$ $\bar{h}h0$ d	A_2B_2 A_3	$00l$ $l=4n+2$ d	A_3			$2h'+l'=4n+2$ d	A_2B_2 A_3
110 $I4_1cd$			$hh0$ $\bar{h}h0$ d	A_2B_2 A_3	$00l$ $l=4n+2$ d	A_3	c	A_2B_2 A_3	$2h'+l'=4n+2$ d	A_2B_2 A_3

respectively. Similarly, when the lattice type C is combined with the a- or b-glide plane in the (001) plane, GM lines are not produced in the $h00$ or $0k0$ (h and k odd) reflections, respectively. The case of the lattice type B is omitted. For example, space groups $Abm2$ and $Cmma$ come under this heading.

6. The incident beam is assumed to impinge so as to form GM lines by a screw axis or a glide plane. Another glide plane is assumed to be present perpendicular to the incident beam and its glide translation is not perpendicular to the screw axis or to the glide translation of the former glide plane (Fig. 2). In such a case the two-dimensional GM lines A_2 and B_2 due to the screw axis or the former glide plane are not produced, since the latter glide plane prohibits *Umweganregung* routes in the zeroth Laue zone to excite the forbidden reflections due to the former symmetry elements. An example is the space group $P2_1/a\bar{3}$, in which only the B_3 GM line is produced at the [100] electron incidence by the 2_1 axis lying in the [010] direction.

Dynamic extinction tables

Using the dynamic extinction rules described in the previous section, we have examined all space groups for which GM lines A_2, A_3, B_2 and B_3 are formed at various crystal settings. For the examination, we postulate that the atoms occupy the general positions of a space group and do not consider the forbidden reflections caused by the special positions. We have to consult the full symbols of space groups, otherwise we may overlook some glide planes and screw axes.

The results are shown in Tables 2 to 16. The space groups are written in the first column of the tables. The expected GM lines are shown for various incident-beam directions in the following columns. We give details in the following examples which are necessary to understand the tables. For instance, the intersection of the third row and the fourth column in Table 3 shows that two-dimensional GM lines A_2 and B_2 and the three-dimensional GM line B_3 are produced at [001] electron incidence in the odd-order $h00$ and $0k0$ reflections by the 2_1 screw axes of space group $P2_12_12$. The second suffixes 1 and 2 of the symbols 2_{11} and 2_{12} distinguish between the first (in the **a** direction) and the second (in the **b** direction) scew axes of the space group. The glide symbols in the second column for space group $P4/nnc$ (Table 10) have two suffixes (n_{21} and n_{22}). The first suffix 2 denotes the second glide plane between two n-glide planes of the space group. The second suffixes 1 and 2, which appear in the tetragonal and cubic systems, distinguish two equivalent glide planes which lie in the x and y planes. The equivalent planes are

Table 9. *GM lines for point group* $\bar{4}2m$

Space group	Incident beam direction [100]		[001]		[110]		[0kl]		[hhl]	
111 $P\bar{4}2m$										
112 $P\bar{4}2c$					$00l$ c	A_3			$h'h'l'$ c	A_2B_2 A_3
113 $P\bar{4}2_1m$	$0k0$ 2_{12}	A_2B_2 B_3	$h00$ 2_{11} $0k0$ 2_{12}	A_2B_2 B_3			$h00$ 2_1	A_2B_2 B_3		
114 $P\bar{4}2_1c$	$0k0$ 2_{12}	A_2B_2 B_3	$h00$ 2_{11} $0k0$ 2_{12}	A_2B_2 B_3	$00l$ c	A_3	$h00$ 2_1	A_2B_2 B_3	c	A_2B_2 A_3
115 $P\bar{4}m2$										
116 $P\bar{4}c2$	$00l$ c_2	A_3					$0k'l'$ c	A_2B_2 A_3		
117 $P\bar{4}b2$			$h00$ b_2 $0k0$ b_1	A_2B_2 A_3			$0k'l'$ b	A_2B_2 A_3		
118 $P\bar{4}n2$	$00l$ n_2	A_3	$h00$ n_2 $0k0$ n_1	A_2B_2 A_3			$0k'l'$ n	A_2B_2 A_3		
119 $I\bar{4}m2$										
120 $I\bar{4}c2$							$0k'l'$ c	A_2B_2 A_3		
121 $I\bar{4}2m$										
122 $I\bar{4}2d$			$hh0$ $\bar{h}h0$ d	A_2B_2 A_3	$00l$ $l=4n+2$ d	A_3			$2h'+l'=4n+2$ d	A_2B_2 A_3

	Space group	[100]		[001]		[110]		[0kl]		[hhl]		[hk0]	
123	$P4/mmm$ $P4/m2/m2/m$												
124	$P4/mcc$ $P4/m2/c2/c$	$00l$ c_{12}	A_3			$00l$ c_2	A_3	$0k'l'$ c_1	A_2B_2 A_3	$h'h'l'$ c_2	A_2B_2 A_3		
125	$P4/nbm$ $P4/n2/b2/m$	$0k0$ n	A_3	$h00$ b_2 $0k0$ b_1	A_3			$0k'l'$ b	A_2B_2 A_3			$\bar{k}h0$ n	A_2B_2 A_3
126	$P4/nnc$ $P4/n2/n2/c$	$0k0$ n_1 $00l$ n_{22}	A_3	$h00$ n_{22} $0k0$ n_{21}	A_3	$00l$ c	A_3	$0k'l'$ n_2	A_2B_2 A_3	c	A_2B_2 A_3	n_1	A_2B_2 A_3
127	$P4/mbm$ $P4/m2_1/b2/m$	$0k0$ 2_{12}	B_3	$h00$ $b_2, 2_{11}$ $0k0$ $b_1, 2_{12}$	A_2B_2 A_3B_3			$0k'l'$ b $h00$ 2_1	A_2B_2 A_3 A_2B_2 B_3				
128	$P4/mnc$ $P4/m2_1/n2/c$	$00l$ n_2 $0k0$ 2_{12}	A_3 B_3	$h00$ $n_2, 2_{11}$ $0k0$ $n_1, 2_{12}$	A_2B_2 A_3B_3	$00l$ c	A_3	$0k'l'$ n $h00$ 2_1	A_2B_2 A_3 A_2B_2 B_3	c	A_2B_2 A_3		
129	$P4/nmm$ $P4/n2_1/m2/m$	$0k0$ $n, 2_{12}$	A_2B_2 A_3B_3	$h00$ 2_{11} $0k0$ 2_{12}	B_3			$h00$ 2_1	A_2B_2 B_3			n	A_2B_2 A_3
130	$P4/ncc$ $P4/n2_1/c2/c$	$0k0$ $n, 2_{12}$ $00l$ c_{12}	A_2B_2 A_3B_3 A_3	$h00$ 2_{11} $0k0$ 2_{12}	B_3	$00l$ c_2	A_3	$0k'l'$ c_1 $h00$ 2_1	A_2B_2 A_3 A_2B_2 B_3	c_2	A_2B_2 A_3	n	A_2B_2 A_3
131	$P4_2/mmc$ $P4_2/m2/m2/c$					$00l$ c	A_3			c	A_2B_2 A_3		
132	$P4_2/mcm$ $P4_2/m2/c2/m$	$00l$ c_2	A_3					$0k'l'$ c	A_2B_2 A_3				
133	$P4_2/nbc$ $P4_2/n2/b2/c$	$0k0$ n	A_3	$h00$ b_1 $0k0$ b_2	A_3	$00l$ c	A_3	$0k'l'$ b	A_2B_2 A_3	c	A_2B_2 A_3	n	A_2B_2 A_3
134	$P4_2/nnm$ $P4_2/n2/n2/m$	$0k0$ n_1 $00l$ n_{22}	A_3	$h00$ n_{22} $0k0$ n_{21}	A_3			$0k'l'$ n_2	A_2B_2 A_3			n_1	A_2B_2 A_3
135	$P4_2/mbc$ $P4_2/m2_1/b2/c$	$0k0$ 2_{12}	B_3	$h00$ $b_2, 2_{11}$ $0k0$ $b_1, 2_{12}$	A_2B_2 A_3B_3	$00l$ c	A_3	$0k'l'$ b $h00$ 2_1	A_2B_2 A_3 A_2B_2 B_3	c	A_2B_2 A_3		
136	$P4_2/mnm$ $P4_2/m2_1/n2/m$	$00l$ n_2 $0k0$ 2_{12}	A_3 B_3	$h00$ $n_2, 2_{11}$ $0k0$ $n_1, 2_{12}$	A_2B_2 A_3B_3			$0k'l'$ n $h00$ 2_1	A_2B_2 A_3 A_2B_2 B_3				
137	$P4_2/nmc$ $P4_2/n2_1/m2/c$	$0k0$ $n, 2_{12}$	A_2B_2 A_3B_3	$h00$ 2_{11} $0k0$ 2_{12}	B_3	$00l$ c	A_3	$h00$ 2_1	A_2B_2 B_3	c	A_2B_2 A_3	n	A_2B_2 A_3
138	$P4_2/ncm$ $P4_2/n2_1/c2/m$	$0k0$ $n, 2_{12}$ $00l$ c_2	A_2B_2 A_3B_3 A_3	$h00$ 2_{11} $0k0$ 2_{12}	B_3			$0k'l'$ c $h00$ 2_1	A_2B_2 A_3 A_2B_2 B_3			n	A_2B_2 A_3
139	$I4/mmm$ $I4/m2/m2/m$												
	$I4/mcm$												

Table 10. (*cont.*)

Space group	Incident beam direction [100]		[001]		[110]		[0*kl*]		[*hhl*]		[*hk*0]	
141 $I4_1/amd$ $I4_1/a2/m2/d$			*hh*0 $\bar{h}h0$ *d*	A_3	00*l* $l = 4n + 2$ *d* $\bar{h}h0$ *a*	A_3			$2h' + l' = 4n + 2$ *d*	A_2B_2 A_3	*a*	A_2B_2 A_3
142 $I4_1/acd$ $I4_1/a2/c2/d$			*hh*0 $\bar{h}h0$ *d*	A_3	00*l* $l = 4n + 2$ *d* $\bar{h}h0$ *a*	A_3	$0k'l'$ *c*	A_2B_2 A_3	$2h' + l' = 4n + 2$ *d*	A_2B_2 A_3	*a*	A_2B_2 A_3

Table 11. *GM lines for point groups* 3, $\bar{3}$, 32 *and* 3*m*

Space groups Nos. 143–155 no GM line.

Space group	Incident beam direction [11$\bar{2}$0]		[1$\bar{1}$00]	
156 *P*3*m*1				
157 *P*31*m*				
158 *P*3*c*1			00*l* *c*	A_2B_2 A_3
159 *P*31*c*	00*l* *c*	A_2B_2 A_3		
160 *R*3*m*				
161 *R*3*c*			00*l* $l = 6n + 3$ *c*	A_2B_2 A_3
162 $P\bar{3}1m$				
163 $P\bar{3}1c$	00*l* *c*	A_2B_2 A_3		
164 $P\bar{3}m1$				
165 $P\bar{3}c1$			00*l* *c*	A_2B_2 A_3
166 $R\bar{3}m$				
167 $R\bar{3}c$			00*l* $l = 6n + 3$ *c*	A_2B_2 A_3

distinguished only for the cases of [100], [010] and [001] electron incidences, for convenience. The *c*-glide planes of space group *Pcc*2 (Table 4) are distinguished by the symbols c_1 and c_2, since the equivalent planes are not present. The glide symbol in the third column for space group *P*4/*mbm* (Table 10) has a suffix 1 or 2. The suffix distinguishes the equivalent glide planes lying in the *x* and *y* planes. Another suffix is not necessary, since the space group has only one *b* symbol. When the index of the incident-beam direction is represented only by a letter like the [*h*0*l*] in Table 2, the index *h* or *l* can take the value zero. That is, the GM-line rules are applicable to [100] and [001] electron incidences. However, if the columns for [100], [010] and [001] incidences are present, as in Table 4, [*hk*0], [0*kl*] and [*h*0*l*] incidences cover only the incidences of non-zero *h*, *k* and *l*. The reflections in which GM lines appear are always perpendicular to the corresponding incident-beam directions ($0k'l'$ $\perp$[0*kl*], $h'k'0$ $\perp$[*hk*0],...). The indices of the reflections in which GM lines appear are odd, if no remark is given. For *c*-glide planes of space groups *R*3*c* and $R\bar{3}c$ and for a *d*-glide plane, the reflections in which GM lines appear are specified as $6n + 3$ and $4n + 2$ orders, respectively.

It is found from the tables that 191 space groups can be distinguished by the difference in the GM lines appearing for various electron incidences. It is assumed that the lattice types *P*, *C*, *I* and *F* are determined kinematically. It is noted that the handedness is determined by a different method (Goodman & Johnson, 1977; Goodman & Secomb, 1977). The 16 pairs of space groups which cannot be distinguished by GM lines are enumerated in Table 17. These indistinguishable pairs have to be identified from the intensity change of the forbidden reflections by varying crystal orientation. An example is the pair *I*4 and $I4_1$. If the intensity of the 200 reflection diminishes or decreases appreciably by varying crystal orientation, the space group is identified to be $I4_1$.

Experimental results

Identification of screw axis and glide plane

If the three-dimensional GM lines are observed, it is obvious whether the GM lines are produced from a screw axis or from a glide plane. As a result, the space groups can be determined by using the tables given in the previous section. It is, however, not easy to observe the three-dimensional GM lines, since broad two-dimensional GM lines appear. In order to distinguish between these symmetry elements, Steeds, Rackham & Shannon (1978) proposed two methods which utilize the three-dimensional symmetries appearing in the transmitted beam and examine how the two-dimensional GM lines change on rotating the crystal, instead of observing the three-dimensional GM lines. However, these methods are disadvantageous from the experimental viewpoint, since they require two photographs taken at different crystal settings.

We emphasize that the presence of the three-dimensional GM lines can be revealed by inspecting the symmetries of the fine lines due to higher Laue-zone reflections in a forbidden reflection in place of the direct observation of the GM lines and the methods of Steeds *et al.* That is, if the fine lines form GM lines, these lines must be symmetric with respect to the two-dimensional GM lines, and *vice versa*. This method which uses the symmetries of fine lines can find the three-dimensional GM lines easily and requires only one photograph. In most cases, the fine lines can be generated when relatively thick areas of a crystal are examined. Fig. 3 shows the CBED patterns taken from thin (*a*) and thick (*b*) areas of FeS_2, of which the space group is $P2_1/a\bar{3}$, with [100] electron incidence. In Fig. 3(*a*), the pattern of the first-order reflection which is set at the Bragg condition is composed of broad GM lines due to two-dimensional interaction. On the other hand, the fine lines due to three-dimensional interaction are clearly seen in Fig. 3(*b*). The fine lines are symmetric with respect to both the A_2 and B_2 GM lines (Fig. 3*b*). This fact proves the presence of the A_3 and B_3 GM

Table 12. *GM lines for point groups* 6, $\bar{6}$, $6/m$, 622, $6mm$, $\bar{6}m2$ *and* $6/mmm$

Space group	Incident beam direction $[11\bar{2}0]$		$[1\bar{1}00]$	
168 $P6$				
169 $P6_1$	$00l$ 6_1	A_2B_2 B_3	$00l$ 6_1	A_2B_2 B_3
170 $P6_5$	$00l$ 6_5	A_2B_2 B_3	$00l$ 6_5	A_2B_2 B_3
171 $P6_2$				
172 $P6_4$				
173 $P6_3$	$00l$ 6_3	A_2B_2 B_3	$00l$ 6_3	A_2B_2 B_3
174 $P\bar{6}$				
175 $P6/m$				
176 $P6_3/m$	$00l$ 6_3	A_2B_2 B_3	$00l$ 6_3	A_2B_2 B_3
177 $P622$				
178 $P6_122$	$00l$ 6_1	A_2B_2 B_3	$00l$ 6_1	A_2B_2 B_3
179 $P6_522$	$00l$ 6_5	A_2B_2 B_3	$00l$ 6_5	A_2B_2 B_3
180 $P6_222$				
181 $P6_422$				
182 $P6_322$	$00l$ 6_3	A_2B_2 B_3	$00l$ 6_3	A_2B_2 B_3
183 $P6mm$				
184 $P6cc$	$00l$ c_2	A_3	$00l$ c_1	A_3
185 $P6_3cm$	$00l$ 6_3	B_3	$00l$ $6_3, c$	A_2B_2 A_3B_3
186 $P6_3mc$	$00l$ $6_3, c$	A_2B_2 A_3B_3	$00l$ 6_3	B_3
187 $P\bar{6}m2$				
188 $P\bar{6}c2$			$00l$ c	A_2B_2 A_3
189 $P\bar{6}2m$				
190 $P\bar{6}2c$	$00l$ c	A_2B_2 A_3		
191 $P6/mmm$				
192 $P6/mcc$	$00l$ c_2	A_3	$00l$ c_1	A_3
193 $P6_3/mcm$	$00l$ 6_3	B_3	$00l$ $6_3, c$	A_2B_2 A_3B_3
194 $P6_3/mmc$	$00l$ $6_3, c$	A_2B_2 A_3B_3	$00l$ 6_3	B_3

(*a*)

(*b*)

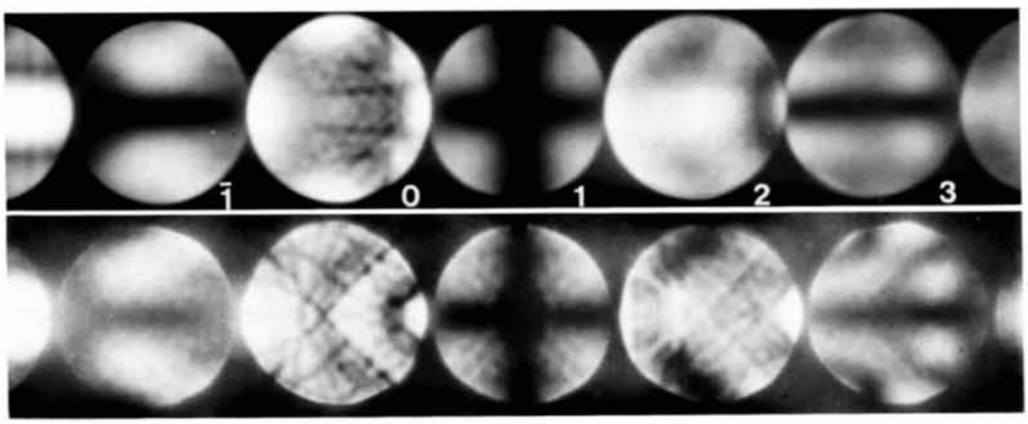

Fig. 3. CBED patterns of FeS_2 taken from (*a*) thin and (*b*) thick areas with [100] incidence: only broad fringes due to two-dimensional interaction are seen in the first-order disk in (*a*), whereas fine lines due to three-dimensional interaction can also be seen in (*b*). Symmetry of fine lines with respect to broad fringes can determine the symmetry elements.

Table 13. *GM lines for point groups* 23 *and* $m3$

Space group	Incident beam direction [100] (cyclic)		[hk0] (cyclic)	
195 $P23$				
196 $F23$				
197 $I23$				
198 $P2_13$	$00l$ 2_{13} $0k0$ 2_{12}	A_2B_2 B_3	$00l$ 2_1	A_2B_2 B_3
199 $I2_13$				
200 $Pm3$ $P2/m\bar{3}$				
201 $Pn3$ $P2/n3$	$00l$ n_2 $0k0$ n_3	A_3	$\bar{k}h0$ n	A_2B_2 A_3
202 $Fm3$ $F2/m3$				
203 $Fd3$ $F2/d\bar{3}$	$00l$ $l = 4n + 2$ d_2 $0k0$ $k = 4n + 2$ d_3	A_3	$\bar{k}h0$ $h + k$ $= 4n + 2$ d	A_2B_2 A_3
204 $Im3$ $I2/m\bar{3}$				
205 $Pa3$ $P2_1/a\bar{3}$	$00l$ $a_2, 2_{13}$ $0k0$ 2_{12}	A_2B_2 A_3B_3 B_3	$00l$ 2_1 $\bar{k}h0$ a	A_2B_2 B_3 A_2B_2 A_3
206 $Ia3$ $I2_1/a3$			$\bar{k}h0$ a	A_2B_2 A_3

Table 14. *GM lines for point group* 432

Space group	Incident beam direction [0kl] (cyclic)	
207 $P432$		
208 $P4_232$		
209 $F432$		
210 $F4_132$		
211 $I432$		
212 $P4_332$	$h00$ 4_{31}	A_2B_2 B_3
213 $P4_132$	$h00$ 4_{11}	A_2B_2 B_3
214 $I4_132$		

Table 15. *GM lines for point group* $\bar{4}3m$

Space group	Incident beam direction [100] (cyclic)		[110] (cyclic)		[hhl] (cyclic)	
215 $P\bar{4}3m$						
216 $F\bar{4}3m$						
217 $I\bar{4}3m$						
218 $P\bar{4}3n$			$00l$ n	A_3	$h'h'l'$ n	A_2B_2 A_3
219 $F\bar{4}3c$					c	A_2B_2 A_3
220 $I\bar{4}3d$	$0kk$ $0kk$ d	A_2B_2 A_3	$00l$ $l = 4n + 2$ d	A_3	$2h' + l'$ $= 4n + 2$ d	A_2B_2 A_3

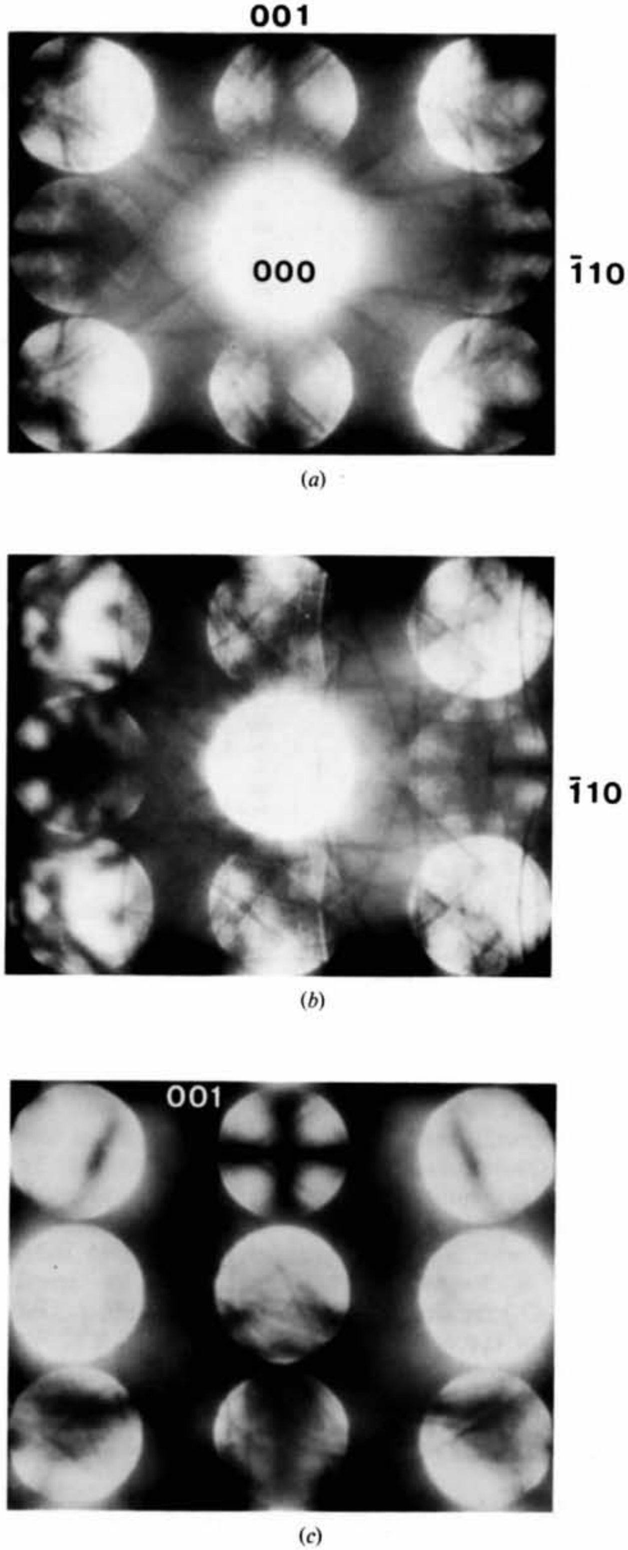

Fig. 4. CBED patterns of FeS_2 taken with [110] incidence: (*a*) zone-axis pattern; (*b*) and (*c*) the 110 and 001 reflections are set at Bragg condition, respectively. A_3 and B_3 lines due to *a*-glide plane and 2_1 screw axis are separately observed in the $\bar{1}10$ and 001 disks, respectively

Table 16. *GM lines for point group m3m*

Space group	Incident beam direction [100] (cyclic)		[110] (cyclic)		[0*kl*] (cyclic)		[*hhl*] (cyclic)	
221 $Pm3m$ $P4/m\bar{3}2m$								
222 $Pn3n$ $P4/n32/n$	$00l$ n_{12} $0k0$ n_{13}	A_3	$00l$ n_2	A_3	$0\bar{l}k$ n_1	$A_2\,B_2$ A_3	$h'h'l'$ n_2	$A_2\,B_2$ A_3
223 $Pm3n$ $P4_2/m\bar{3}2/n$			$00l$ n	A_3			n	$A_2\,B_2$ A_3
224 $Pn3m$ $P4_2/n\bar{3}2/m$	$00l$ n_2 $0k0$ n_3	A_3			n	$A_2\,B_2$ A_3		
225 $Fm3m$ $F4/m\bar{3}2/m$								
226 $Fm3c$ $F4/m\bar{3}2/c$							c	$A_2\,B_2$ A_3
227 $Fd3m$ $F4_1/d\bar{3}2/m$	$00l$ $l = 4n + 2$ d_2 $0k0$ $k = 4n + 2$ d_3	A_3			$k + l = 4n + 2$ d	$A_2\,B_2$ A_3		
228 $Fd3c$ $F4_1/d32/c$	$00l$ $l = 4n + 2$ d_2 $0k0$ $k = 4n + 2$ d_3	A_3			$k + \bar{l} = 4n + 2$ d	$A_2\,B_2$ A_3	$h'h'l'$ c	$A_2\,B_2$ A_3
229 $Im3m$ $I4/m\bar{3}2/m$								
230 $Ia3d$ $I4_1/a32/d$	$0kk$ $0\bar{k}k$ d	A_3	$00l$ $l = 4n + 2$ d $\bar{h}h0$ a_3	A_3	a	$A_2\,B_2$ A_3	$2h' + l' = 4n + 2$ d	$A_2\,B_2$ A_3

lines, or of an a-glide plane and a 2_1 screw axis. For such an examination, the fine lines must be formed near the positions where the GM lines are produced. To satisfy this condition for any crystals, it is desirable that the accelerating voltage of the incident beam is variable with a step of about a few hundred volts. Steeds & Evans (1980) demonstrated for spinel ($MgAl_2O_4$) the change of the fine lines forming A_3 GM lines with the accelerating voltage near 100 kV. We observed at 40, 60 and 80 kV that the fine lines from spinel appear far from the positions where the GM lines are produced.

Separation between GM lines due to screw axis and those due to glide plane

In Fig. 3, the A_3 line due to an a-glide plane and the B_3 line due to a 2_1 screw axis are simultaneously observed in the 001 disk. Table 13 shows that A_3 and B_3 lines can be separately observed in the $\bar{k}h0$ and $00l$ reflections with $[hk0]$ electron incidence. Fig 4 demonstrates the theoretical results by experiment. Fig. 4(a) shows a [110] zone-axis CBED pattern of FeS_2. The A_2 lines are seen in both the 001 and $\bar{1}10$ disks. By observing the symmetry of fine lines due to higher Laue-zone reflections, it is found that the A_3 line is produced in the $\bar{1}10$ reflection but is not produced in the 001 reflection. Thus, the a-glide plane is detected in the $\bar{1}10$ reflection and the 2_1 screw axis in the 001

Table 17. *Space groups indistinguishable by GM lines*

($P3$, $P3_1$, $P3_2$)	($P4/m$, $P4_2/m$)
($P312$, $P3_112$, $P3_212$)	($P4/n$, $P4_2/n$)
($P321$, $P3_121$, $P3_221$)	($P422$, $P4_222$)
($P6$, $P6_2$, $P6_4$)	($P42_12$, $P4_22_12$)
($P622$, $P6_222$, $P6_4\,22$)	($I4$, $I4_1$)
($P6_3$, $P6_1$, $P6_5$)	($I422$, $I4_122$)
($P6_322$, $P6_122$, $P6_522$)	($I23$, $I2_13$)
($P4$, $P4_2$)	($I222$, $I2_12_12_1$)

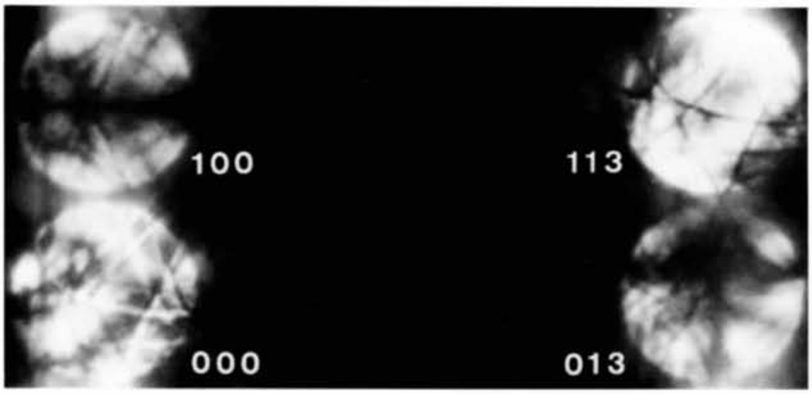

Fig. 5. Symmetrical four-beam CBED pattern of FeS_2. The 100, 013 and 113 reflections are set at Bragg conditions. B_2 and B_3 lines are seen in the 100 disk, and only the B_2 line in 013 disk.

reflection. It is noted that the A_2 line in the 001 reflection is somewhat obscured by the fine lines which do not form an A_3 line.

To confirm the result, two CBED patterns were taken at the $\bar{1}10$ and 001 Bragg settings (Figs. 4*b* and *c*). The fine lines are symmetric with respect to the A_2 line in the $\bar{1}10$ reflection (Fig. 4*b*), and are symmetric with respect to the B_2 line in the 001 reflection (Fig. 4*c*). This confirms again that the A_3 line due to an *a*-glide plane and the B_3 line due to a 2_1 screw axis are formed in the $\bar{1}10$ and 001 reflections, respectively.

GM lines in a symmetrical many-beam pattern

The tables given in the previous section are applicable to the cases in which the projection of the Laue point is present at the midpoint of the line connecting the transmitted beam and the forbidden reflection. In the symmetrical many-beam CBED patterns (Tanaka, Saito & Sekii, 1983), the GM-line rules are modified. However, the new tables for the symmetrical many-beam cases are not necessary, since the modification is not complicated. The modification is understood for an example of GM lines in a symmetrical four-beam pattern from FeS_2 (Fig. 5). The 100, 013 and 113 reflections are set at Bragg conditions in the pattern. The B_2 and B_3 lines are produced in the 100 reflection. This shows the presence of a 2_1 screw axis in the [100] direction. To this reflection, the GM-line rules given in the column of the [*hk*0] electron incidence for the space group $P2_1/a\bar{3}$ (Table 13) is still applicable, since the crystal rotation about a screw axis is not effective for detecting the screw axis (Steeds, Rackham & Shannon, 1978). Only the B_2 line is seen in the 013 disk, although it is obscured by the fine lines. The GM-line rules cannot be applicable to this reflection, since the rules require the appearance of A_2 and A_3 lines. The *A* lines appear only when the incident beam lies in a glide plane. In the present case, the condition is not satisfied. The B_2 line can still appear, since glide plane and 2_1 screw axis act identically in the two-dimensional interaction and two *Umweganregung* routes (*a*) and (*c*) shown in the paper of Gjønnes & Moodie (1965) are set at the same diffraction condition.

The authors thank Mr F. Sato for his technical assistance.

References

COWLEY, J. M. & MOODIE, A. F. (1959). *Acta Cryst.* **12**, 360–367.

COWLEY, J. M., MOODIE, A. F., MIYAKE, S., TAKAGI, S. & FUJIMOTO, F. (1961). *Acta Cryst.* **14**, 87–88.

FUJIWARA, K. (1959). *J. Phys. Soc. Jpn*, **14**, 1513–1524.

GJØNNES, J. & MOODIE, A. F. (1965). *Acta Cryst.* **19**, 65–67.

GOODMAN, P. & JOHNSON, A. W. S. (1977). *Acta Cryst.* A**33**, 997–1001.

GOODMAN, P. & SECOMB, T. W. (1977). *Acta Cryst.* A**33**, 126–133.

MIYAKE, S., TAKAGI, S. & FUJIMOTO, F. (1960). *Acta Cryst.* **13**, 360–361.

STEEDS, J. W. & EVANS, N. S. (1980). *Proc. Electron Microsc. Soc. Am.*, edited by G. W. BAILEY, pp. 188–191. Barton Rouge: Claitor.

STEEDS, J. W., RACKHAM, G. M. & SHANNON, M. D. (1978). *Inst. Phys. Conf. Ser.* **41**, 135–139.

TANAKA, M., SAITO, R. & SEKII, H. (1983). *Acta Cryst.* A**39**, 357–368.

TANAKA, M. & SEKII, H. (1982*a*) *Tenth Int. Congr. Electron Microscopy, Hamburg*, pp. 631–632.

TANAKA, M. & SEKII, H. (1982*b*). Preprints of the Spring Meeting of the Physical Society of Japan, Yokohama, April, pp. 2–388.

TINNAPPEL, A. (1975). PhD Thesis, Tech. Univ. Berlin.